Materials Research Proceedings 34 (2023) 237-245 https://doi.org/10.21741/9781644902691-28

Numerical Analysis of a Pneumatic Cushion Operation Safety, including the Airflow Conditions

FILO Grzegorz[1, a *] and LEMPA Paweł[1,b]

[1]Cracow University of Technology, Kraków, Poland

[a]grzegorz.filo@pk.edu.pl, [b]pawel.lempa@pk.edu.pl

Keywords: Pneumatic Cushion, Heavy Load Movement, Air Velocity, Critical Air Flow, Numerical Modelling, Matlab, Simulink

Abstract. This work concerns studying the characteristics of a pneumatic cushion in a system for moving heavy loads. Particular emphasis has been placed on the airflow parameters through the main supply nozzle, including the average flow velocity. Critical flow at the speed of sound can occur under certain circumstances. In the subsequent steps, a mathematical model of a pneumatic cushion was formulated, next, a simulation model was built in the Matlab/Simulink system, and then numerical simulations were carried out. As a result, it was estimated whether there is a flow with a safe, appropriately low speed in a given range of load and supply pressure.

Introduction

The indoor transport of heavy loads is a common problem in many industrial companies. The movement must be carried out quickly and efficiently. Various transportation devices, such as cranes, forklifts, or conveyors, can be used for this purpose. Sometimes a beneficial alternative may be using transport platforms on pneumatic cushions [1, 2]. They are particularly convenient under the safety requirements regarding the inability to use combustion engines and electrical devices. The simple and compact design allows the cushions to be easily inserted under bulky loads or devices, even heavy ones or of enormous dimensions. The handy feature is their small height of approximately 30 – 40 mm. However, using air cushion systems requires specific requirements to be met. Firstly, access to an air supply system with a certain pressure and flow rate must be provided. In addition, the operating floor must be suitably smooth and level, including the inclination $\alpha \leq 0.1^0$ and the roughness $R_a \leq 12.5$ μm [3, 4]. When the air supply is turned on, a thin film is formed between the lower plane of the cushion and the ground. The film is created by the air radially flowing out of the chamber located in the central part. It reduces the friction coefficient between the cushion and the ground to approximately $\mu = 0.001$.

In the standard design of a pneumatic cushion [2, 5, 6], the air flows through a nozzle located centrally in the cushion axis. An important issue is ensuring proper outflow uniformity and estimating the required parameters of the air supply system. The phenomena accompanying the flow of gases are complex; therefore, they are the subject of research in many research centres. The issue of the work includes modelling and numerical analyses of elements and systems such as pneumatic cylinders [7], pneumatic vibration isolation systems with multiple air chambers [8] or air springs [9]. Another crucial issue is the appropriate control of the airflow rate. The manufacturers usually provide manual control systems. Nevertheless, the possibility of using automatic controllers with advanced algorithms, such as fuzzy logic [10] or pulse width modulation (PWM) technique [11], is also being investigated. The aim of the research is often a reduction in energy consumption [12] or an increase in the efficiency of the system [13].

This paper deals with the issue of ensuring the safety of a pneumatic cushion operation by analysing the speed of airflow through the supply nozzle. The built model and numerical simulations carried out in the Matlab/Simulink system were aimed at estimating whether, given

Materials Research Proceedings 34 (2023) 237-245 https://doi.org/10.21741/9781644902691-28

the power supply parameters and load values, there would appear conditions for the formation of a critical flow with the speed of sound.

Reliability and safety of pneumatic devices are of paramount importance as potential failures can pose a threat to the health and lives of workers, especially in high-pressure conditions [14-16]. Therefore, it is necessary to develop scenarios for potential failures [17-19], prevent them, and mitigate their consequences when they occur. This places a requirement on the devices and their individual working components to exhibit high-quality characteristics [20-22].

The main risk factors for failures are equipment wear [23-25], failures of structural joints, including welded joints [26-28], and unwanted gas and liquids ingress [29-31]. Preventing failures requires the use of materials with desired technological and functional properties [32-34], and in specific cases, complementing them with coatings that modify their characteristics [35], including coatings with special functional properties [36-38] and those that alter mechanical properties [39-41]. Additionally, the morphology of the surface layer can be modified by changing frictional conditions [42-44]. The complexity of methods and the multifactorial nature of processes necessitate the application of dimensionality reduction techniques [45,46] and process optimization methods [47-49], including nonparametric techniques [50,51]. Ultimately, in conjunction with FMEA scenarios, this enables a reduction in the required resources [52].

In addition to the primary benefits of increased reliability and safety, it also leads to lower energy consumption [53], thereby increasing the applicability of pneumatic cushion transporters, both as standalone systems and as part of larger devices [54-56], posing competition to typical wheeled or conveyor-based transportation [57]. The military has long recognized the advantages of such transportation, especially in the case of air-cushion landing crafts [58-60].

Working Principle of a Pneumatic Cushion

The analysed pneumatic cushion is based on a DELU 4LTM-200-1 type (fig. 1). It consists of a rigid aluminium plate (2) with four landing pads (3). In the lower part, there are rubber bellows (4) of a shape similar to a torus. The air flows through the inlet port (1) and the nozzle (5) to the central chamber of the V_1 volume. The cushion has the following nominal operational parameters: input pressure p_0 = 2.4 bar, and the air consumption Q_0 = 180 dm^3/min.

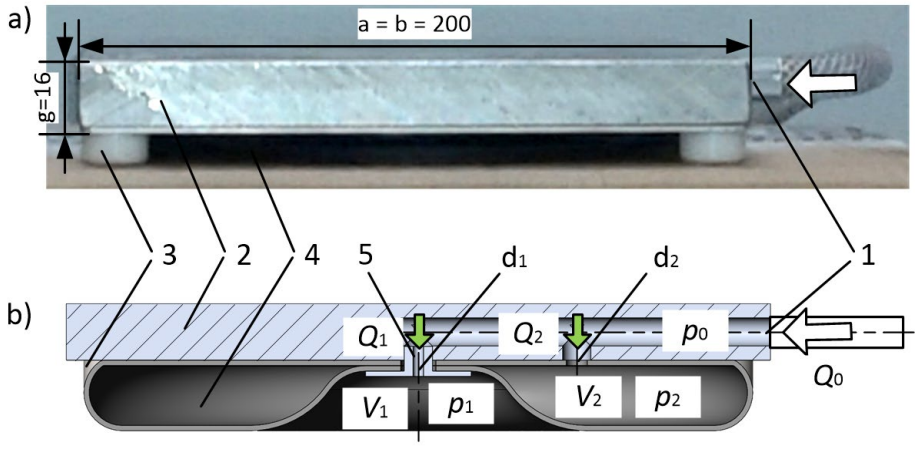

Fig. 1 Pneumatic cushion: (a) real cushion, b) cross-section through the 3D model; 1 – inlet port, 2 – aluminium plate, 3 – landing pad, 4 – rubber bellows, 5 – nozzle

After opening the airflow, the p_1 pressure appears at the inlet. Air flows into the central chamber of V_1 volume through the d_1 nozzle and simultaneously into the bellows through the d_2 nozzle. After some time, the bellows fill up, and the flow occurs through the d_1 nozzle. When the p_1 pressure reaches a sufficiently high value, the gap between the lower surface of the bellows and the ground is formed, and the outflow to the atmosphere begins. The pressure difference

Materials Research Proceedings 34 (2023) 237-245 https://doi.org/10.21741/9781644902691-28

$\Delta p = p_0 - p_1$ is established, which determines the Q_1 flow rate through the nozzle and, thus, the average velocity of the air stream.

The mass stream $\dot{m}_1(t)$ of air flowing into the central chamber through the d_1 nozzle can be determined by taking into account the critical velocity of the flow [5, 6]. The air velocity depends on the pressure ratio p_1 / p_0. In the case of assuming an adiabatic change during the flow (omission heat exchange with the environment), the threshold value of this coefficient is constant and equal to $\beta_0 = 0.53$. If the value of the pressure ratio $p_1 / p_0 \le \beta_0$, which means $p_1 \le 0.53 \cdot p_0$, the supercritical flow occurs at the speed of sound, otherwise the flow velocity is lower. Hence, the equation of the air inflow to the V_1 volume can be written as follows:

$$\frac{dm_1(t)}{dt} = \frac{\pi \cdot d_1^2}{4} \cdot p_0(t) \cdot \sqrt{\frac{2}{R \cdot T_0}} \cdot \Psi(t), \tag{1}$$

where T_0 is air temperature at the inlet, the specific air constant $R = 287\ J/(kg \cdot K)$ and the $\psi(t)$ coefficient for the subcritical flow (heat capacity ratio κ=1.4) is determined from the relation ([6]):

$$\psi(t) = \sqrt{\frac{\kappa}{\kappa - 1}\left[\left(\frac{p_1(t)}{p_0(t)}\right)^{2/\kappa} - \left(\frac{p_1(t)}{p_0(t)}\right)^{(\kappa+1)/\kappa}\right]}. \tag{2}$$

In the case of supercritical flow, the coefficient ψ has a constant value of $\psi_{crit} = 0.684$. Hence, the equation (1) is simplified to the following form:

$$\frac{dm_1(t)}{dt} = 0.7594 \cdot \frac{d_1^2 \cdot p_0(t)}{\sqrt{R \cdot T_0}}. \tag{3}$$

The volumetric flow rate can be determined by dividing the mass flow by the air density:

$$Q_1(t) = \frac{1}{\rho} \cdot \frac{dm_1(t)}{dt}, \tag{4}$$

and thus the average velocity of the air stream is:

$$v_{av}(t) = \frac{4Q_1(t)}{\pi \cdot d_1^2}. \tag{5}$$

The mathematical model also includes equations related to the V_2 chamber flow, bottom gap formation, payload, equation of motion in the vertical direction, etc. The complete model the one can find in the publication [1].

Simulink Model and Numerical Analysis

The created simulation model in the form of a Simulink block diagram is shown in fig. 2. It includes subsystems for an input step function U_in, a relief valve INLET_VALVE, two nozzles d1_nozzle, d2_nozzle and two chambers V1_chamber, V2_chamber, respectively. Signals are related to p_0, p_1, p_2 pressures, dm1/dt, dm2/dt flow rates, z_f, z_2 heights of the air gap and the bellows, V_2 chamber volume and v_1_avg flow velocity through the nozzle. The results are stored in a file using a Results_to_file block.

Materials Research Proceedings 34 (2023) 237-245 https://doi.org/10.21741/9781644902691-28

The test plan assumed checking the flow velocity through the nozzle d1 for the load values in the $F_{load} = 100, 500, 1500, 2500$ N and the supply pressure $p_0 = 1.2, 1.8, 2.4$ bar. The first step determined the velocity for different load values at a fixed supply pressure. Next, simulations were carried out at different pressure values for the fixed load force. Fig. 3 and fig. 4 show the results obtained in the first and the second step, respectively.

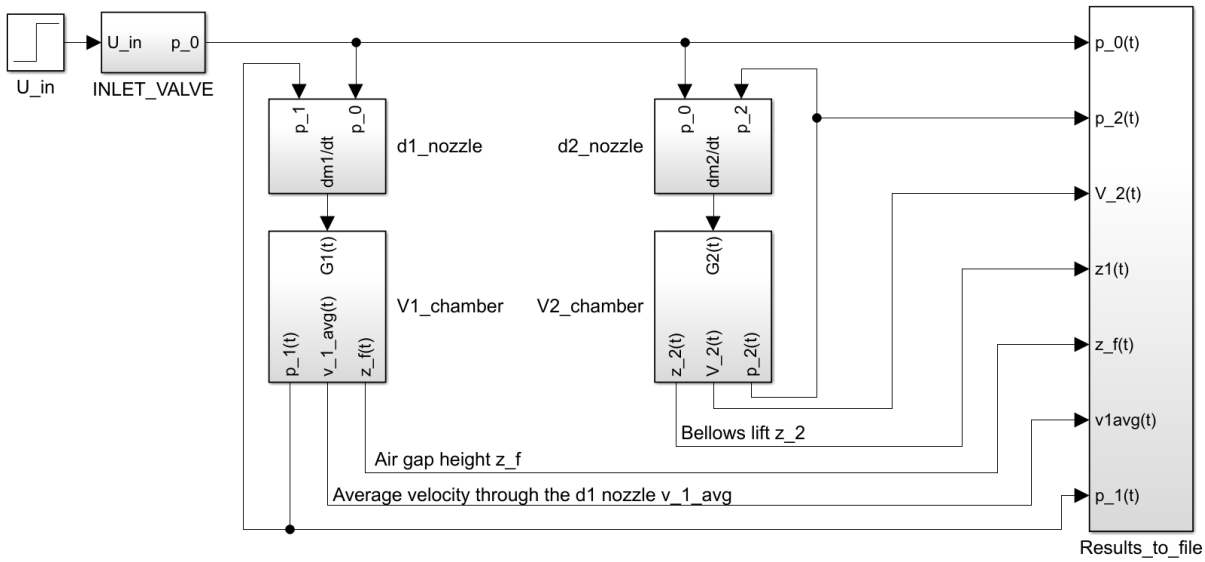

Fig. 2 Block diagram of a Simulink model

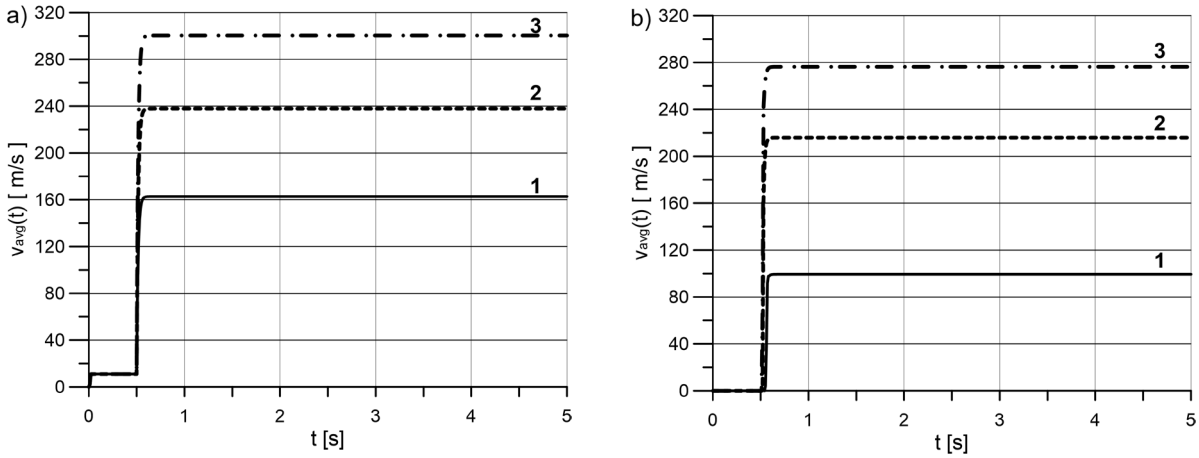

Fig. 3 Air velocity for fixed load force value: a) F_{load} = 100 N, b) F_{load} = 1500 N; 1 – p_0 = 1.2 bar, 2 – p_0 = 1.8 bar, 3 – p_0 = 2.4 bar

Materials Research Proceedings 34 (2023) 237-245 https://doi.org/10.21741/9781644902691-28

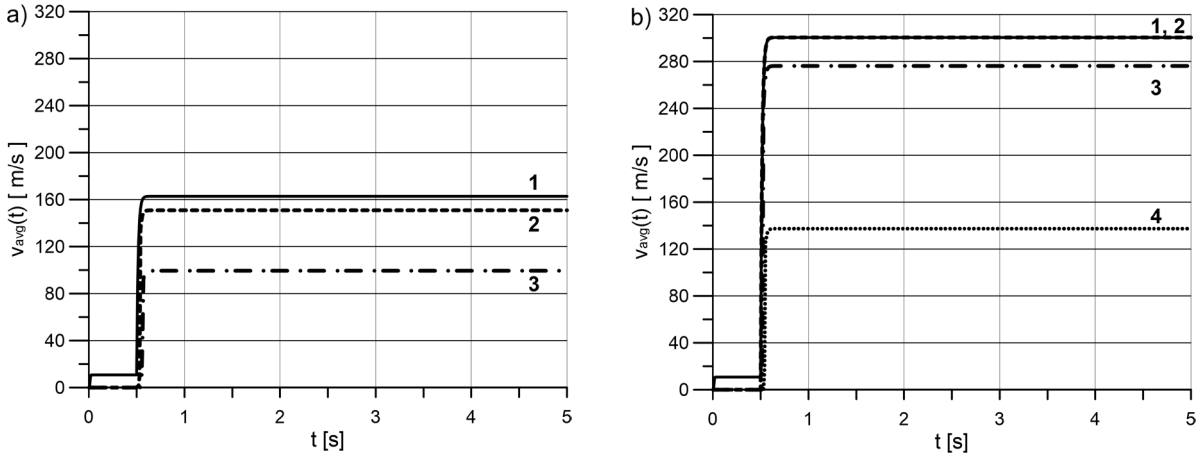

Fig. 4 Air velocity for fixed input pressure: a) p_0 = 1.2 bar, b) p_0 = 2.4 bar; 1 – F_{load} = 100 N, 2 – F_{load} = 500 N, 3 – F_{load} = 1500 N, 4 – F_{load} = 2500 N

Fig. 3 shows that the velocity value for F_{load} =100 N is in the range between 160 and 295 m/s, while for F_{load} = 1500 N, between 100 and 275 m/s, respectively. In the case of F_{load} =2500 N, the air film was formed only at the pressure p_0 = 2.4 bar, and in this case, the velocity value 137 m/s was obtained. As arises from fig. 4, at a supply pressure of 1.2 bar, the velocity value ranges from 100 to 160 m/s, and the maximum load force is 1500 N. When the supply pressure is 2.4 bar, the obtained air velocity varies from 140 to 295 m/s, respectively.

Summary

The article aimed to conduct a numerical analysis of the parameters of a pneumatic cushion intended for use in heavy load handling systems. In particular, it was checked whether the conditions of critical flow formation with the speed of sound could occur in the air supply nozzle. The simulations in Simulink showed that the highest air flow velocity occurs when the maximum supply pressure is set at minimum load. However, the maximum flow velocity obtained is less than 300 m/s. In practice, putting the full airflow at minimum payload can occur with manual pressure setting and may be prevented by applying an automatic control system.

References

[1] E. Lisowski, G. Filo. Automated heavy load lifting and moving system using pneumatic cushions, Autom. Constr. 50 (2015) 91-101. https://doi.org/10.1016/j.autcon.2014.12.004.

[2] E. Lisowski, D. Kwiatkowski. Determination of basic parameters of pneumatic transport platform system with pneumatic bags, Przegląd Mechaniczny 12(2) (2012) 45-48.

[3] K. Kaya, O. Özcan. A numerical investigation on aerodynamic characteristics of an air-cushion vehicle. J. Wind Eng. Ind. Aerodyn. 120 (2013) 70-80. https://doi.org/10.1016/j.jweia.2013.06.012.

[4] E. Lisowski, D. Kwiatkowski. Nonlinear static analysis of air cushion in SolidWorks Simulation 2016. Technical Transactions 115 (2018) 211-218. https://doi.org/10.4467/2353737XCT.18.030.8003

[5] J. Wołkow, R. Dindorf. Teoria i obliczenia układów pneumatycznych. Wydawnictwo Politechniki Krakowskiej, Kraków, 1994.

[6] W. Szejnach. Napęd i sterowanie pneumatyczne. WNT, Warszawa, 2003. ISBN 8320429188

[7] D.N. Dihovicni, M. Medenica. Simulation, Analyze and Program Support for Pneumatic Cylinder System. Proc. WCE 2009 World Cong. Engin., Vol I, 149-152. ISBN: 9789881701251

[8] J.-H. Moon, B.-G. Lee. Modeling and sensitivity analysis of a pneumatic vibration isolation system with two air chambers. Mechanism and Machine Theory 45 (2010) 1828-1850. https://doi.org/10.1016/j.mechmachtheory.2010.08.006.

[9] T. Bešter, M. Fajdiga, M. Nagode. Application of Constant Amplitude Dynamic Tests for Life Prediction of Air Springs at Various Control Parameters. Strojniški Vestnik/Journal of Mechanical Engineering 60 (2014) 241-249. https://doi.org/10.5545/sv-jme.2013.1348

[10] E. Lisowski, G. Filo. Pressure control in air cushions of the mobile platform. Journal of KONES Powertrain and Transport 18 (2011) 261-270.

[11] A. Messina, N. Giannoccaro, A. Gentile. Experimenting and modeling the dynamics of pneumatic actuators controlled by the pulse width modulation (PWM) technique. Mechatronics 15 (2005) 859-881. https://doi.org/10.1016/j.mechatronics.2005.01.003

[12] R. Dindorf. Estimating Potential Energy Savings in Compressed Air Systems. Procedia Engineering 39 (2012) 204-211. https://doi.org/10.1016/j.proeng.2012.07.026

[13] E. Richer, Y. Hurmuzlu. A high performance pneumatic force actuator system :part 1 - nonlinear mathematical model. J. Dyn. Syst. Meas. Control 122 (2000) 416-425. https://doi.org/10.1115/1.1286336

[14] G. Barucca et al. The potential of Λ and Ξ- studies with PANDA at FAIR, Europ. Phys. J. A 57 (2021) art.154 https://doi.org/10.1140/epja/s10050-021-00386-y

[15] M. Domagala et al. CFD Estimation of a Resistance Coefficient for an Egg-Shaped Geometric Dome, Appl. Sci. 12 (2022) art.10780. https://doi.org/10.3390/app122110780

[16] M. Domagala et al. The Influence of Oil Contamination on Flow Control Valve Operation, Mater. Res. Proc. 24 (2022) 1-8. https://doi.org/10.21741/9781644902059-1

[17] J. Fabiś-Domagała et al. Instruments of identification of hydraulic components potential failures, MATEC Web of Conf. 183 (2018) art.03008. https://doi.org/10.1051/matecconf/201818303008

[18] K. Knop et al. Evaluating and Improving the Effectiveness of Visual Inspection of Products from the Automotive Industry, Lecture Notes in Mechanical Engineering (2019) 231-243. https://doi.org/10.1007/978-3-030-17269-5_17

[19] J. Fabis-Domagala et al. A concept of risk prioritization in FMEA analysis for fluid power systems, Energies 14 (2021) art. 6482. https://doi.org/10.3390/en14206482

[20] R. Ulewicz, F. Nový. Quality management systems in special processes, Transp. Res. Procedia 40 (2019) 113-118. https://doi.org/10.1016/j.trpro.2019.07.019

[21] D. Siwiec et al. Improving the non-destructive test by initiating the quality management techniques on an example of the turbine nozzle outlet, Materials Research Proceedings 17 (2020) 16-22. https://doi.org/10.21741/9781644901038-3

[22] K. Czerwinska et al. Improving quality control of siluminial castings used in the automotive industry, METAL 2020 29th Int. Conf. Metall. Mater. (2020) 1382-1387. https://doi.org/10.37904/metal.2020.3661

[23] S. Marković et al. Exploitation characteristics of teeth flanks of gears regenerated by three hard-facing procedures, Materials 14 (20210 art. 4203. https://doi.org/10.3390/ma14154203

[24] M. Krynke et al. Maintenance management of large-size rolling bearings in heavy-duty machinery, Acta Montan. Slovaca 27 (2022) 327-341. https://doi.org/10.46544/AMS.v27i2.04

[25] P. Regulski, K.F. Abramek. The application of neural networks for the life-cycle analysis of road and rail rolling stock during the operational phase, Technical Transactions 119 (2022) art. e2022002. https://doi.org/10.37705/TechTrans/e2022002

[26] M. Patek et al. Non-destructive testing of split sleeve welds by the ultrasonic TOFD method, Manuf. Technol. 14 (2014) 403-407. https://doi.org/10.21062/ujep/x.2014/a/1213-2489/MT/14/3/403

[27] N. Radek, J. Pietraszek, A. Goroshko. The impact of laser welding parameters on the mechanical properties of the weld, AIP Conf. Proc. 2017 (2018) art.20025. https://doi.org/10.1063/1.5056288"

[28] N. Radek et al. Properties of Steel Welded with CO2 Laser, Lecture Notes in Mechanical Engineering (2020) 571-580. https://doi.org/10.1007/978-3-030-33146-7_65

[29] M. Ulewicz et al. Ion flotation of zinc(II) and cadmium(II) in the presence of side-armed diphosphaza-16-crown-6 ethers, Sep. Sci. Technol. 38 (2003) 633-645. https://doi.org/10.1081/SS-120016655

[30] M. Zenkiewicz, T. Zuk, J. Pietraszek, P. Rytlewski, K. Moraczewski, M. Stepczyńska. Electrostatic separation of binary mixtures of some biodegradable polymers and poly(vinyl chloride) or poly(ethylene terephthalate), Polimery/Polymers 61 (2016) 835-843. https://doi.org/10.14314/polimery.2016.835

[31] T. Zuk et al. Modeling of electrostatic separation process for some polymer mixtures, Polymers 61 (2016) 519-527. https://doi.org/10.14314/polimery.2016.519

[32] P. Szataniak, F. Novy, R. Ulewicz. HSLA steels - Comparison of cutting techniques, METAL 2014 - 23rd Int. Conf. Metallurgy and Materials (2014), Ostrava, Tanger, 778-783.

[33] D. Klimecka-Tatar, M. Ingaldi. Assessment of the technological position of a selected enterprise in the metallurgical industry, Mater. Res. Proc. 17 (2020) 72-78. https://doi.org/10.21741/9781644901038-11

[34] P. Jonšta et al. The effect of rare earth metals alloying on the internal quality of industrially produced heavy steel forgings, Materials 14 (2021) art.5160. https://doi.org/10.3390/ma14185160

[35] W. Zórawski et al. Plasma-sprayed composite coatings with reduced friction coefficient, Surf. Coat. Technol. 202 (2008) 4578-4582. https://doi.org/10.1016/j.surfcoat.2008.04.026

[36] N. Radek et al. Microstructure and tribological properties of DLC coatings, Mater. Res. Proc. 17 (2020) 171-176. https://doi.org/10.21741/9781644901038-26

[37] N. Radek et al. Influence of laser texturing on tribological properties of DLC coatings, Prod. Eng. Arch. 27 (2021) 119-123. https://doi.org/10.30657/pea.2021.27.15

[38] N. Radek et al. Operational properties of DLC coatings and their potential application, METAL 2022 31st Int. Conf. Metall. Mater. (2022) 531-536. https://doi.org/10.37904/metal.2022.4491

[39] N. Radek, J. Konstanty. Cermet ESD coatings modified by laser treatment, Arch. Metall. Mater. 57 (2012) 665-670. https://doi.org/10.2478/v10172-012-0071-y

[40] N. Radek et al. The effect of laser treatment on operational properties of ESD coatings, METAL 2021 30th Ann. Int. Conf. Metall. Mater. (2021) 876-882. https://doi.org/10.37904/metal.2021.4212

[41] N. Radek et al. The impact of laser processing on the performance properties of electro-spark coatings, 14th World Congress in Computational Mechanics and ECCOMAS Congress 1000 (2021) 1-10. https://doi.org/10.23967/wccm-eccomas.2020.336

[42] N. Radek et al. The WC-Co electrospark alloying coatings modified by laser treatment, Powder Metall. Met. Ceram. 47 (2008) 197-201. https://doi.org/10.1007/s11106-008-9005-7

[43] N. Radek et al. Laser Processing of WC-Co Coatings, Mater. Res. Proc. 24 (2022) 34-38. https:10.21741/9781644902059-6

[44] P. Kurp, H. Danielewski. Metal expansion joints manufacturing by a mechanically assisted laser forming hybrid method – concept, Technical Transactions 119 (2022) art. e2022008. https://doi.org/10.37705/TechTrans/e2022008

[45] J. Pietraszek et al. The principal component analysis of tribological tests of surface layers modified with IF-WS2 nanoparticles, Solid State Phenom. 235 (2015) 9-15. https://doi.org/10.4028/www.scientific.net/SSP.235.9

[46] J. Pietraszek, E. Skrzypczak-Pietraszek. The uncertainty and robustness of the principal component analysis as a tool for the dimensionality reduction. Solid State Phenom. 235 (2015) 1-8. https://doi.org/10.4028/www.scientific.net/SSP.235.1

[47] R. Dwornicka, J. Pietraszek. The outline of the expert system for the design of experiment, Prod. Eng. Arch. 20 (2018) 43-48. https://doi.org/10.30657/pea.2018.20.09

[48] J. Pietraszek, N. Radek, A.V. Goroshko. Challenges for the DOE methodology related to the introduction of Industry 4.0. Prod. Eng. Arch. 26 (2020) 190-194. https://doi.org/10.30657/pea.2020.26.33

[49] B. Jasiewicz et al. Inter-observer and intra-observer reliability in the radiographic measurements of paediatric forefoot alignment, Foot Ankle Surg. 27 (2021) 371-376. https://doi.org/10.1016/j.fas.2020.04.015

[50] J. Pietraszek. The modified sequential-binary approach for fuzzy operations on correlated assessments, LNAI 7894 (2013) 353-364. https://doi.org/10.1007/978-3-642-38658-9_32

[51] J. Pietraszek et al. Non-parametric assessment of the uncertainty in the analysis of the airfoil blade traces, METAL 2017 26th Int. Conf. Metall. Mater. (2017) 1412-1418. ISBN 978-8087294796

[52] A. Maszke, R. Dwornicka, R. Ulewicz. Problems in the implementation of the lean concept at a steel works - Case study, MATEC Web of Conf. 183 (2018) art.01014. https://doi.org/10.1051/matecconf/201818301014

[53] Ł.J. Orman. Enhancementof pool boiling heat transfer with pin-fin microstructures, J. Enhanc. Heat Transf. 23 (2016) 137-153. https://doi.org/10.1615/JEnhHeatTransf.2017019452

[54] A. Goroshko et al. Construction and practical application of hybrid statistically-determined models of multistage mechanical systems, Mechanika 20 (2014) 489-493. https://doi.org/10.5755/j01.mech.20.5.8221

[55] R. Ulewicz, M. Mazur. Economic aspects of robotization of production processes by example of a car semi-trailers manufacturer, Manuf. Technol. 19 (2019) 1054-1059. https://doi.org/10.21062/ujep/408.2019/a/1213-2489/MT/19/6/1054

[56] I. Drach et al. Design Principles of Horizontal Drum Machines with Low Vibration, Adv. Sci. Technol. Res. J. 15 (2021) 258-268. https://doi.org/10.12913/22998624/136441

[57] N. Radek, R. Dwornicka. Fire properties of intumescent coating systems for the rolling stock, Commun. - Sci. Lett. Univ. Zilina 22 (2020) 90-96. https://doi.org/10.26552/com.C.2020.4.90-96

[58] W. Przybył et al. Virtual Methods of Testing Automatically Generated Camouflage Patterns Created Using Cellular Automata, Mater. Res. Proc. 24 (2022) 66-74. https://doi.org/10.21741/9781644902059-11

[59] N. Radek et al. Operational tests of coating systems in military technology applications, Eksploat. i Niezawodn. 25 (2023) art.12. https://doi.org/10.17531/ein.2023.1.12

[60] W. Przybył et al. Microwave absorption properties of carbonyl iron-based paint coatings for military applications, Def. Technol. 22 (2023) 1-9. https://doi.org/10.1016/j.dt.2022.06.013